Multi-Trait Improvement by Predicting Genetic Correlations in Breeding Crosses

Jeffrey L. Neyhart, Aaron J. Lorenz, and Kevin P. Smith

Department of Agronomy and Plant Genetics, University of Minnesota, St. Paul, MN 55108

Running title: Predicting genetic correlations

Keywords: genetic correlation, genomewide prediction, cross selection, simulation, barley

Corresponding author:

Kevin P. Smith

411 Borlaug Hall

1991 Upper Buford Circle

St. Paul, Minnesota 55108

Email: smith376@umn.edu

Telephone: +1 (612) 624-1211

ABSTRACT

The many quantitative traits of interest to plant breeders are often genetically correlated, which can complicate progress from selection. Improving multiple traits may be enhanced by identifying parent combinations – an important breeding step – that will deliver more favorable genetic correlations (r_G). Modeling the segregation of genomewide markers with estimated effects may be one method of predicting r_G in a cross, but this approach remains untested. Our objectives were to: (i) specify the theory to predict r_G in a potential cross; (ii) use simulations to assess the accuracy of genomewide predictions of r_G and the long-term response to selection when selecting crosses on the basis of such predictions; and (iii) empirically measure the ability to predict genetic correlations using data from a barley (*Hordeum vulgare* L.) breeding program. We extended previous theory to predict r_G between two traits in a population of inbred lines. Using simulations, we found that the accuracy to predict r_G was generally moderate and strongly influenced by trait heritability, population size, and genetic correlation architecture (i.e. pleiotropy or linkage disequilibrium). Among 26 barley (*Hordeum vulgare* L.) breeding populations, the empirical prediction accuracy of r_G was low (-0.012) to moderate (0.42), depending on the complexity of a trait pair. Within a simulated long-term plant breeding program, selecting crosses based on predicted r_G increased multi-trait genetic gain by 6.0-8.4% compared to selection on the predicted cross mean. Prioritizing crosses based on predicted genetic correlation can be a feasible and effective method of improving unfavorably correlated traits in breeding programs.

INTRODUCTION

Quantitative traits often exhibit complex relationships with one another, with ramifications for disease epidemiology, evolutionary processes, and plant and animal improvement. These relationships may manifest as genetic correlations, which can be caused by shared genetic influence (i.e. pleiotropy) or the non-random association of alleles (i.e. linkage disequilibrium) (Lynch and Walsh 1998). Investigations in quantitative genetics commonly assume that many loci of small effect govern traits [i.e. "infinitesimal model" (Fisher 1919)]. This suggest that a large proportion of the genome should contribute to phenotypic variation, a hypothesis that has been supported by recent genome-wide analyses of complex traits (Mackay 2010; Boyle *et al.* 2017). If true for multiple complex traits, a natural corollary follows that pleiotropy or close linkage of trait-specific genes is widespread. Recent studies attempting to identify quantitative trait loci (QTL) influencing multiple traits using dense genomewide markers have provided support for this idea, reporting extensive pleiotropy or strong genetic correlations (Korte *et al.* 2012; Lee *et al.* 2012; Bulik-Sullivan *et al.* 2015; Schaid *et al.* 2016; Deng and Pan 2017).

Plant breeders routinely select on multiple traits, but progress can be complicated by genetic correlations. If two traits are favorably correlated, selection can simultaneously improve both by tandem selection, indirect selection, or a trait index (Bernardo 2010). Unfavorable correlations, meanwhile, are common and often the bane of the breeder. In crop improvement, notorious examples include grain yield and grain protein content in wheat (*Triticum aestivum* L.; Simmonds 1995), grain yield and plant height in maize (*Zea mays* L.; Chi *et al.* 1969), and seed protein and oil content in soybean (*Glycine max* L.; Bandillo *et al.* 2015). The directions of such correlations imply an unfavorable response in one trait when selecting on another (Falconer and Mackay 1996), and the underlying cause will impact the prospects of long-term improvement.

Selection on traits with shared, antagonistic genetic influence is functionally constrained, but correlations induced by linkage disequilibrium are transient and can be disrupted by recombination (Falconer and Mackay 1996; Lynch and Walsh 1998).

Genomewide selection has become popular among plant breeders as a method of predicting the merit of unphenotyped individuals using genomewide markers and a phenotyped training population (Meuwissen *et al.* 2001). Typical prediction models are univariate (i.e. one trait), but multivariate models have recently been explored as a means of borrowing information from genetically correlated traits and improving the prediction accuracy of both traits (Calus and Veerkamp 2011; Jia and Jannink 2012). Selection on multiple traits using predicted breeding values would proceed as if using phenotypic values, relying on procedures such as tandem selection, independent culling levels, or the construction of a trait index (Bernardo 2010), with most studies of multi-trait genomewide selection using the latter (Combs and Bernardo 2013; Beyene *et al.* 2015; Sleper and Bernardo 2018; Tiede and Smith 2018).

These models and selection methods implicitly assume that the breeding population has already been developed from selected parents. Therefore, the genetic variance of each trait, and the genetic correlation between traits, both of which determine the direct or correlated response to selection (Falconer and Mackay 1996), are fixed parameters of the population. In addition to more accurate selection within an established population, multi-trait genetic gain could be increased by developing better populations through deliberate selection of parent combinations with a more ideal mean, larger genetic variance, and more favorable genetic correlation. Typically, breeders select parents using the expected population mean, which can reliably be predicted as the mean of the two parents (Bernardo 2010). Recently developed methods that rely on *in silico* simulations (Bernardo 2014; Mohammadi *et al.* 2015) or deterministic equations

(Zhong and Jannink 2007; Lehermeier *et al.* 2017; Osthushenrich *et al.* 2017) have been proposed to predict the genetic variance in a potential cross. These procedures model the expected segregation of genomewide markers with estimated effects, and early validation experiments suggest that such procedures may be useful (Lian *et al.* 2015; Tiede *et al.* 2015; Osthushenrich *et al.* 2017; Neyhart and Smith 2019).

Predictions of the population mean and genetic variance could be used to discriminate among potential crosses on the basis of the expected mean of selected progeny in those crosses. This can be quantified by the usefulness criterion (Schnell and Utz 1975), or the superior progeny mean (Zhong and Jannink 2007). The superior progeny mean assumes selection on a single trait, yet if two traits are genetically correlated, a response to selection would also be expected in a second trait. This "correlated progeny mean," as we will refer to it, could be used to further distinguish ideal crosses as long as the genetic correlation is known or can be predicted. Though much research has focused on predicting the genetic variance in breeding crosses (e.g. Souza and Sorrells 1991; Bohn *et al.* 1999; Utz *et al.* 2001), little work has addressed predicting the genetic correlation. The simulation approach codified by Mohammadi *et al.* (2015) generates such predictions, but their accuracy and utility remain unexplored, and the use of simulations can be computationally burdensome for a large number of potential crosses.

The objectives of this study were to (i) specify the theory to predict the genetic correlation between two traits in a potential cross and how crosses may be distinguished by the correlated response of superior progeny; (ii) use simulations to assess the accuracy of genomewide predictions of genetic correlations and the long-term response to selection when selecting crosses on the basis of superior/correlated progeny means; and (iii) empirically measure

the ability to predict genetic correlations using data from a barley (*Hordeum vulgare* L.) breeding program.

METHODS AND MATERIALS

Theory

Below, we first outline a deterministic prediction of the genetic variance of a single trait and the correlation between traits in a recombinant inbred line (RIL) population assuming two fully inbred parents, bi-allelic QTL, and no dominance or epistasis. This derivation follows the notation presented in Zhong and Jannink (2007); others have determined equations for the expected genetic variance in bi-parental populations of intermediate selfing generations (Lehermeier *et al.* 2017) or multi-parent populations (Allier *et al.* 2019), and our derivation could be extended to such mating schemes. We then use these predictions to determine the superior progeny mean and correlated progeny mean for a cross.

Suppose that $L_{(k)}$ QTL influence the kth quantitative trait; in the mth cross, $L_{m(k)}$ QTL are segregating for that trait (where $L_{m(k)} \leq L_{(k)}$). The expected genetic variance in the cross is the sum of the variance of each locus plus the covariance between pairs of loci. As noted in Zhong and Jannink (2007), the genetic variance in cross m is

$$\sigma^2_{G(m)} = \sum_{i=1}^{L_m} \alpha_i^2 + 2\sum_{i<j} \frac{1-2c_{ij}}{1+2c_{ij}} \alpha_i \alpha_j, \tag{1}$$

where α_i and α_j are the allele substitution effects of the ith and jth loci, respectively and c_{ij} is the recombination fraction between the ith and jth loci. Note that in a bi-parental RIL population, the expected allele frequencies at each segregating QTL are $p_i = q_i = 0.5$, so these terms are omitted. As expected, loci that are genetically unlinked (i.e. independent, $c_{ij} = 0.5$) will have a covariance of 0. The covariance can be generalized across coupling and repulsion phase linkage by setting the allele substitution effects $+\alpha_i$ and $+\alpha_j$ to those of the first parent and $-\alpha_i$ and $-\alpha_j$ to those of the second parent (Zhong and Jannink 2007).

The single-trait covariance term in Equation (1) can be modified to calculate the expected genetic covariance between two quantitative traits:

$$\sigma_{G(1,2)(m)} = \sum_{i=1}^{L_{m(1)}} \sum_{j=1}^{L_{m(2)}} \frac{1 - 2c_{i(1)j(2)}}{1 + 2c_{i(1)j(2)}} \alpha_{i(1)} \alpha_{j(2)}\,, \tag{2}$$

where $c_{i(1)j(2)}$ is the recombination fraction between the *i*th locus of trait 1 and the *j*th locus of trait 2, $\alpha_{i(1)}$ is the allele substitution effect of the *i*th locus of trait 1 and $\alpha_{j(2)}$ is the allele substitution effect of the *j*th locus of trait 2. Using the expected genetic variance of each trait calculated from Equation (1) and the expected covariance between traits from Equation (2), the expected genetic correlation is

$$r_{G(1,2)(m)} = \frac{\sigma_{G(1,2)(m)}}{\sqrt{\sigma^2_{G(1)(m)} \sigma^2_{G(2)(m)}}}. \tag{3}$$

With estimates of the genetic variance for two traits and the genetic correlation between the traits, we can rely on established theory to estimate the superior progeny mean ($\mu_{sp(m)}$) and correlated progeny mean in a cross. For trait 1, assumed under direct selection, the superior progeny mean is

$$\mu_{sp(1)(m)} = \mu_{(1)(m)} + k_{sp} \sigma_{G(1)(m)}, \tag{4}$$

where $\mu_{(1)(m)}$ is the expected mean of trait 1 in the cross (estimated as the mean breeding value of the parents) and k_{sp} is the standardized selection coefficient. It is worth noting that the deviation from $\mu_{(1)(m)}$ in Equation (4) is the same as the direct response to selection, $R_{(1)} = k_{sp}\sigma_{G(1)}$, when the heritability is 1. The correlated response of the second trait, after selection on the first, is $CR^{C}_{(2)} = k_{sp} r_{G(1,2)} \sigma_{G(2)}$, which, when expressed as a deviation from the expected mean of the second trait, becomes the correlated progeny mean:

$$\mu^{C}_{sp(2)(m)} = \mu_{(2)(m)} + k_{sp} r_{G(1,2)} \sigma_{G(2)(m)}. \quad (5)$$

As with phenotypic values of two traits in a population, estimates of the superior progeny mean and correlated progeny mean could be used to select crosses that maximize the genetic gain for both traits, through independent culling levels or index selection (Bernardo 2010).

The equations above assume that the loci under consideration are the true QTL influencing the quantitative traits. Since the effects of such QTL are usually unknown, the estimates effects of genomewide markers in linkage disequilibrium with QTL can be used to make predictions. This is the basis of *in silico* methods to predict genetic variance and genetic correlation, such as the R package *PopVar* (Mohammadi *et al.* 2015). The advantage of the deterministic equations is computational speed (about 130-fold faster, data not shown), with a high or perfect correlation between predicted values (Figure S1).

Simulations

We conducted two simulations to assess the utility of predicting the genetic correlation in a breeding cross. Our simulations were based on observed marker genotypes of 1,570 North American two-row spring barley lines genotyped with 3,072 single nucleotide polymorphism (SNP) markers (Close *et al.* 2009), with genetic positions according to a consensus linkage map (Muñoz-Amatriaín *et al.* 2011); all data was obtained from the Triticeae Toolbox (https://triticeaetoolbox.org/barley/; Blake *et al.* 2016). Marker genotypes were arbitrarily coded as -1, 0, 1, where -1 was homozygous for the second allele, 0 was heterozygous, and 1 was homozygous for the first allele. After removing monomorphic and redundant SNPs (identical genotype calls and genetic positions), and SNPs and lines with more than 10% missing data, we were left with a marker matrix of 1,565 lines and 2,309 SNPs. We set the few heterozygous genotypes to missing and imputed missing calls using the mode across each SNP. Additionally,

any SNPs with identical map positions (i.e. due to low genetic resolution) were jittered on the genetic map by 1×10^{-6} cM. These data were used to define the genetic architecture of the simulated quantitative traits and form the initial pool from which to establish a base training population.

Simulation 1 – Accuracy of predicting genetic correlations

The first simulation experiment was designed to assess the conditions influencing the accuracy to predict the genetic correlation in a cross. We perturbed the heritabilities of two traits, the architecture defining the traits (i.e. number of QTL) and genetic correlation, the initial genetic correlation, and the base/training population size (Table 1). Simulations were initiated by drawing 200 SNP markers to act as QTL. For each trait, 100 – L QTL were assigned an effect of 0, where L was the effective number of QTL (30 or 100). QTL effects were defined by a geometric series, as proposed by Lande and Thompson (1990): for the kth QTL, the value of the favorable homozygote was a^k, the value of the heterozygote was 0, and the value of the unfavorable homozygote was $-a^k$, where $a = (1 - L)/(1 + L)$. The first allele at each QTL was randomly assigned to be favorable or unfavorable and larger values were considered favorable for both traits. This randomization was performed independently for each trait.

Genetic correlations were generated according to three different architecture types: pleiotropy, tight linkage, or loose linkage. For simplicity, we assumed that the genetic architecture was governed entirely by one of the types. Under pleiotropy, the sampled QTL effects were first stored in an $L \times 2$ matrix, $\mathbf{A}$. The desired genetic correlation in the base population ($r_{G(0)}$) was achieved by multiplying matrix $\mathbf{A}$ by the Choleski decomposition of the variance-covariance matrix $\mathbf{\Sigma}$, which contained 1 on the diagonal and $r_{G(0)}$ on the off-diagonal. This resulted in a set of QTL with pleiotropic effects that varied in both magnitude and sign for

the two traits. Under tight linkage and loose linkage, each SNP sampled to be an effective QTL for the first trait was paired with another SNP that was sampled – with restrictions – to be an effective QTL for the second trait. For tight linkage, this second SNP was restricted to within 5 cM of the first SNP, and for loose linkage, this second SNP was restricted to between 25 cM and 35 cM of the first SNP. The QTL effects were again stored in the $L \times 2$ matrix **A**, where each row was a pair of QTL, and subsequently adjusted as above. Effects of QTL influencing the second trait were then multiplied by matrix **R**, which contained estimates of linkage disequilibrium (measured as the pairwise correlation, *r*, between genotype states) between QTL influencing the first trait and QTL influencing the second trait. This adjustment resulted in base genetic correlations that approximately matched the target, $r_{G(0)}$ (Figure S2).

The base/training population was first generated by randomly sampling N_{TP} individuals from the simulation starting material. For each trait, the genotypic value of an individual was calculated as the sum of the QTL allele effects carried by that individual, and the genetic variance was calculated as the variance among genotypic values. Phenotypic values were simulated by adding independent normally distributed deviations to the genotypic values to achieve a starting entry-mean heritability of h_p^2 (Table 1) with no residual covariance between traits. Individuals were assumed to be phenotyped in three environments with one replication, and the mean phenotypic value was used for genomewide prediction. Marker effects were predicted using the model $y_{ip} = \mu_p + \sum_{m=1}^{M} x_{im} u_{mp} + \epsilon_{ip}$, where y_{ip} was the phenotypic mean of the *i*th individual for the *p*th trait, μ_p was the population mean for the *p*th trait, x_{im} was the allelic state of the *m*th marker in the *i*th individual, u_{mp} was the predicted effect of the *m*th marker for the *p*th trait, and ϵ_{ip} was the associated error. We used two models to predict marker effects: ridge-regression best linear unbiased prediction (RR-BLUP) and BayesCπ (Habier *et al.*

2011). Potential crosses were generated by randomly sampling 50 pairs of individuals from the base population. We predicted the genetic correlation ($\hat{r}_{G(1,2)}$) for each potential cross using Equations (1), (2), and (3), where α was substituted with u_{mp}. The expected genetic correlation ($r_{G(1,2)}$) was similarly computed but instead using the known QTL effects instead of the predicted marker effects. Prediction accuracy was defined as the correlation between the predicted and expected genetic correlations. As a comparison, we also assessed predictions of the trait-specific mean ($\hat{\mu}_{(p)}$) and genetic variance ($\hat{\sigma}^2_{G(p)}$) in each cross. Each condition of this simulation was replicated 100 times.

Simulation 2 – Correlated response to selection

We conducted a second simulation experiment to measure the long-term response to selection of two correlated traits under different cross selection strategies. The range of perturbed parameters was smaller than in the first simulation (Table 1), though simulations were initiated as described above. We assumed that a breeder wanted to simultaneously increase the genotypic value of two quantitative traits, therefore positive genetic correlations were favorable. The base/training population was created by randomly sampling N_{TP} = 600 individuals from the simulation starting material. Informed by the results of the first simulation (see below), we used only the simpler RR-BLUP model to predict marker effects. Potential parents for the first breeding cycle were selected by determining the best 30 individuals in training population based on an equal-weight index of the normalized predicted genotypic values (Hazel 1943). We predicted the mean, genetic variance, and genetic correlation for all possible non-reciprocal crosses between the potential parents. We then calculated the superior progeny mean of the first trait and the correlated progeny mean of the second trait using the predicted parameters and Equations (4) and (5).

Twenty crosses were selected on the basis of an index of the normalized predicted correlated/superior progeny means $\left(\hat{\mu}_{sp}^{I} = \hat{\mu}_{sp(1)} + \hat{\mu}_{sp(2)}^{C}\right)$, an index of the normalized predicted cross means $\left(\hat{\mu}^{I} = \hat{\mu}_{(1)} + \hat{\mu}_{(2)}\right)$, or random selection. We will subsequently refer to the non-random cross selection methods by their abbreviations: CPM (correlated/superior progeny mean) or FM (family, or cross, mean). From the selected crosses, families of 50 recombinant inbred lines were simulated using the *qtl* R package (Broman *et al.* 2003). Recombination events were sampled according to the genetic map (Muñoz-Amatriaín *et al.* 2011), with the assumption of no crossover interference or mutation. This resulted in a pool of 1,000 selection candidates. Finally, potential parents for the next breeding cycle were chosen from these candidates using predicted genotypic values and the same index as described above. We simulated 10 cycles of recurrent selection (outlined in Figure 1), during which marker effect estimates remained unchanged. Along with the standardized selection response for each trait, we also tracked the genetic variance of each trait, the genetic correlation between traits, the frequency of favorable, unfavorable, and antagonistic (i.e. two alleles with opposite effect) QTL haplotypes, and the proportion of QTL with fixed alleles. Simulation were replicated 250 times, and we report the mean and 95% approximate confidence interval for each measured variable.

Empirical validation

To empirically validate predictions of genetic correlations, we used phenotypic and genotypic data from a barley breeding program. The details of data generation are described elsewhere (Neyhart and Smith 2019), but we include a brief overview below. A training population (TP) of 175 two-row spring barley lines was genotyped with 6,361 SNP markers and phenotyped for heading date (a proxy for flowering time), *Fusarium* head blight (a disease caused by the fungal

pathogen *Fusarium graminearum* Schwabe), and plant height in four environments. The genetic correlation between traits in the TP was estimated using the bi-variate mixed model

$$\mathbf{y} = \boldsymbol{\mu} + \mathbf{Zg} + \mathbf{e}, \tag{6}$$

where $\mathbf{y}$ is a 175 × 2 matrix of genotypic means [i.e. best linear unbiased estimates (BLUEs) from a model accounting for genotype, environment, and genotype-environment interaction] for two traits on 175 lines, $\boldsymbol{\mu}$ is a 1 × 2 vector of trait-specific population means, $\mathbf{Z}$ is an incidence matrix relating phenotypes to lines, $\mathbf{g}$ is a 175 × 2 matrix of trait-specific genotypic values, and $\mathbf{e}$ is a 175 × 2 matrix of residuals (Lee *et al.* 2012). The random genotypic values and residuals were assumed distributed as $\mathbf{g} \sim MVN(0, \mathbf{G} \otimes \boldsymbol{\Sigma})$ and $\mathbf{e} \sim MVN(0, \mathbf{I} \otimes \mathbf{R})$, where $\mathbf{G}$ is the realized genomic relationship matrix, $\mathbf{I}$ is an identity matrix, and $\otimes$ denotes the Kronecker product between matrices. The genotypic and residual covariance structures are

$$\boldsymbol{\Sigma} = \begin{bmatrix} \sigma^2_{G(1)} & \sigma_{G(1,2)} \\ \sigma_{G(1,2)} & \sigma^2_{G(2)} \end{bmatrix}, \tag{7}$$

and

$$\mathbf{R} = \begin{bmatrix} \sigma^2_{e(1)} & \sigma_{e(1,2)} \\ \sigma_{e(1,2)} & \sigma^2_{e(2)} \end{bmatrix}. \tag{8}$$

The genetic correlation was estimated from elements in $\boldsymbol{\Sigma}$ using Equation (3).

Among all potential non-reciprocal crosses between 813 offspring of the TP (n = 330,078), we used the R package *PopVar* to predict the genetic correlation for each pair of traits. (Predictions were generated early in the experiment using this package, so for consistency we used those values, and not those generated using the deterministic equations above.) Twenty-six crosses were made based on the predictions, producing "validation families" ranging from 28 to 160 F_5 lines. Validation families were phenotyped for the same three traits in 2 or 4 environments. Observations of heading date and plant height were recorded for all families, but

due to logistical constraints of the inoculated disease nursery, only 14 families were phenotyped for *Fusarium* head blight severity. Genotypic BLUEs of each line across all environments were used to calculate the observed genetic correlation in each family using Equation (6), with the exception that $\mathbf{G}$ was substituted with an identity matrix. Validation families were ungenotyped and the genetic correlation was calculated on a per-family basis, so a pedigree- or marker-based relationship matrix were not of use. Finally, we measured predictive ability as the correlation between predicted and estimated genetic correlation, and the significance of this coefficient was tested using 1,000 bootstrapping replicates. Note that predictive ability is calculated by comparing predictions with phenotype-based observations, whereas prediction accuracy compares predictions with the true genotypic parameter (unobservable in our empirical experiment).

Data availability

Marker data for initiating the simulations and all data used in the empirical validation experiment is available from the Triticeae Toolbox (T3; https://triticeaetoolbox.org/barley/). All simulations and analyses were performed in R (v. 3.5.1; R Core Team, 2018) and relevant scripts are located in the GitHub repository https://github.com/UMN-BarleyOatSilphium/GenCorPrediction. Instructions are included in this repository for downloading data from T3. Supplementary figures and tables are available through Figshare.

RESULTS

Factors influencing predictions of genetic correlation

In our simulation, prediction accuracy for the genetic correlation in potential crosses was most influenced by trait heritability, training population size (N_{TP}), and genetic architecture. We provide a cross-section of results in Figure 2, and all results for the first simulation are displayed in Figure S3 and Table S1. Accuracy increased additively as a function of the heritability of both simulated traits, but only reached a maximum of about 0.81 under the most ideal conditions (Figure S3, Table S1). On average, accuracy increased by about 1.5-fold when moving from N_{TP} = 150 to N_{TP} = 600. We generally did not observe a pattern of diminishing returns when increasing N_{TP}, though some evidence of that pattern was present under the tight linkage architecture (Figure 2).

Between all correlation architectures, tight linkage resulted in the highest prediction accuracy, followed by loose linkage and then pleiotropy. The difference in accuracy under tight linkage versus loose linkage was on average 0.071 (17%) and this difference under loose linkage versus pleiotropy was 0.017 (6.2%). With tight linkage and loose linkage genetic architectures, accuracy was slightly higher when 100 versus 30 QTL influenced both traits (a difference of about 0.04, or 10%), but the reverse was true under pleiotropy, where the accuracy was about 8% lower (a difference of about 0.03) with more QTL (Figure 2). Interestingly, an interaction was apparent between the genetic architecture and the prediction model. Under pleiotropy and tight linkage, there was a slight advantage to using the BayesCπ model over RR-BLUP, particularly when 30 QTL influenced each trait. This difference was quite slim, however, with a boost to accuracy of only about 0.015 (3%).

The family mean and genetic variance of each trait in potential crosses were almost always predicted with greater accuracy than the genetic correlation (Figure 3, Table S1). In general, the family mean was predicted most accurately, followed by the genetic variance and the genetic correlation. (The genetic variance of one trait was occasionally predicted more accurately than the family mean of another trait, but only if the heritability of the first trait was much less than the second.) This trend was consistent across training population sizes, prediction models, and genetic architectures. The average (and range in) prediction accuracy was 0.87 (0.64, 1.0) for the family mean, 0.66 (0.34, 0.96) for the genetic variance, and 0.48 (0.18, 0.81) for the genetic correlation.

Long-term response with different cross selection strategies

Our second simulation showed that the genetic gain for two correlated quantitative traits was impacted by the base genetic correlation, the genetic architecture, and the strategy to select crosses (Figure 4). We found little difference in the outcome when the heritability of the second trait was 0.6; therefore, we highlight results when the heritability of the second trait was 0.3, a more realistic situation for indirect selection (Bernardo 2010). When measuring progress via a trait index (Figure 4A), we found that selecting crosses based on the predicted correlated superior progeny mean (CPM) resulted in a greater response than selection on the predicted cross mean (FM) or by random selection. Under all genetic architectures, the advantage of imposing non-random cross selection became clear after 1 breeding cycle. Subsequently, after 3 cycles, selecting crosses based on CPM resulting in higher gain than by selecting based on FM. Only after 9 – 10 cycles did random cross selection achieve equivalent or superior genetic gain compared with FM selection, though it never outperformed selection using CPM.

Gain from selection, and marginal differences between selection methods, depended on the genetic architecture and correlation. The final genetic gain was, on average, less when the genetic correlation was negative. With pleiotropic architecture, the reduction in genetic gain from positive to negative correlation was more severe (a roughly 100% decrease) than with tight or loose linkage architectures (a roughly 20% decrease). With one exception, the marginal gain from selection (based on an index) when using CPM versus FM ranged from 0.113 (6.0%) with pleiotropic architecture and negative correlation to 0.32 (8.4%) with pleiotropic architecture and positive correlation. When the correlation was negative and defined by loose linkage architecture, the response with selection using CPM was 0.014 (0.57%) genetic standard deviations less than with selection using FM (Figure 4A).

When considering traits individually, we found that much of the advantage of selecting crosses on CPM was realized in the response of the first trait (Figure 4B). For the second trait, selection on CPM or FM yielded similar responses, except under pleiotropic architecture and a positive genetic correlation. Again, random cross selection led to the lowest response, though in some cases it became equivalent to selection on CPM or FM after 10 breeding cycles. Genetic gain was consistent for the primary trait, with a plateau reached after 6 – 8 cycles of selection. Conversely, we observed a rapid plateauing in the genetic gain of the secondary trait, with onset after 3 – 5 cycles. The only condition in which the response of the secondary trait more closely mirrored that of the primary trait was under pleiotropic architecture and positive genetic correlation.

Changes in variance components and gene frequencies with multi-trait selection

As expected, the genetic variance for both traits decreased over cycles of selection (Figure 5A), and by cycle 10, most had been exhausted. Although genetic variance for the first trait declined

similarly under varying architectures, the loss of variance for the second trait was more precipitous when the architecture was defined by linkage versus pleiotropy. Under the latter, genetic variance for the second trait was reduced at a rate comparable to the first trait (Figure 5A). We found that cross selection by FM always led to the most rapid reduction of genetic variance, while this decay was slower when selecting on CPM and slower yet with random mating. This ranking among selection methods was very apparent for the first trait (and for the second trait under pleiotropic architecture), but marginal differences were much less for the second trait.

The genetic correlation in the breeding population consistently declined in absolute value, moving towards zero under all simulated conditions (Figure 5B). The genetic architecture impacted the rate of change, with the most rapid movement under loose linkage, followed by tight linkage and then pleiotropy, as expected. The correlation initially became more negative when selection was imposed on the base population (i.e. cycle 0 to cycle 1). This change was much larger when the base correlation ($r_{G(0)}$) was positive; indeed, under non-pleiotropic architecture, the genetic correlation became near-zero, or negative, after 1 cycle of selection. Conversely, when $r_{G(0)}$ was negative, the genetic correlation moved more steadily towards 0. For all conditions, we found that selecting crosses on CPM usually led to a more positive genetic correlation than selection on FM, particularly in the first 5 breeding cycles.

Changes in haplotype frequency were greatest when loose linkage defined the correlation architecture, followed by tight linkage and pleiotropy (Figure 6A). The change in haplotype frequencies was more limited with negative $r_{G(0)}$, particularly under pleiotropic architecture. With loose linkage architecture and positive $r_{G(0)}$, we also observed a slightly greater reduction in the frequency of antagonistic haplotypes when selecting crosses by CPM. For the remaining

circumstances, though, this reduction was equivalent when selecting crosses on CPM versus FM. As expected, the frequency of antagonistic haplotypes did not change when the architecture was defined by pleiotropy (Figure 6A). Selection increasingly drove QTL to fixation (Figure 6B), but the rate of fixation was uneven for different cross selection methods. Choosing crosses on FM led to the highest fixation rate, followed by CPM and then random mating. There was a slightly higher fixation rate with positive genetic correlation than with negative genetic correlation, and the fixation rates for QTL influencing the first trait or second trait were equivalent.

Empirical validation of predicted genetic correlations

We used genomewide markers and phenotypic data to empirically estimate the genetic correlation for three pairs of quantitative traits in our 175-line training population (TP). The genetic correlation was -0.99 between *Fusarium* head blight (FHB) severity and heading date, -0.61 between FHB severity and plant height, and 0.38 between heading date and plant height (Table 2). These estimates were reflected in predictions of the cross mean and genetic correlation of 330,078 potential crosses (Figure 7, Table 2). The average predicted genetic correlation among the potential crosses was -0.54 for FHB severity and heading date, -0.26 for FHB severity and plant height, and 0.24 for heading date and plant height. Though the genetic correlations between FHB severity and both heading date and plant height were unfavorable (earlier-flowering, shorter, and disease resistant plants are desirable), predictions implied that progress could be made by selecting populations with more favorable genetic correlations. For instance, more than 2,400 (0.73%) potential crosses were predicted to have a favorable (i.e. positive) correlation between FHB severity and heading date.

The mean (and range) of estimated genetic correlations among the validation families was -0.18 (-0.72, 0.58) for FHB severity and heading date, -0.038 (-0.67, 0.64) for FHB severity

and plant height, and -0.13 (-0.64, 0.69) for heading date and plant height (Table 3). Estimates of predictive ability for genetic correlations ranged from -0.012 to 0.41 (Table 3). We could only validate predictions of the correlation between heading date and plant height, where all 26 validation families (VF) were phenotyped. The predictive abilities for remaining trait combinations were not significantly different from zero ($P > 0.05$; bootstrapping). The ability to predict the genetic correlation appeared to coincide with the heritability of both traits; the entry-mean heritability in the TP (and in the VF) was 0.45 (0.11) for FHB severity, 0.96 (0.78) for heading date, and 0.52 (0.74) for plant height (Neyhart and Smith 2019).

DISCUSSION

Predictions of genetic correlations are feasible with reliable training data

Our first simulation measured the prediction accuracy of genetic correlations as a function of training population (TP) size, trait heritability, prediction model, and genetic architecture. Our results implicated the usual suspects driving genomewide prediction accuracy for individual traits. Increasing the TP size and the heritability of both traits improved accuracy, an expected result given the importance of these parameters (Daetwyler *et al.* 2008; Wimmer *et al.* 2013).

The impact of genetic architecture was curious. Genetic correlations caused by loose linkage or pleiotropy led to lower prediction accuracies compared to architecture defined by tight linkage (Figure 2). We hypothesize that the same phenomenon, albeit with opposite effect, is responsible. Genomewide prediction models (i.e. RRBLUP or BayesCπ) assume that many more markers than true QTL have non-zero effect on both traits. Our approach to predicting genetic correlations relies on the recombination and segregation of these markers, implying that all contribute to variability in genetic variance and covariance, while only true QTL generate this variability. With pleiotropy, this would manifest as a downward bias in the covariance between traits, as we predict a greater possibility of recombination between markers than what is possible for the true QTL. Under loose linkage, an opposite, upward bias in covariance would be expected, as the many markers with uneven trait effects would be predicted to co-segregate more often than what is possible for the true QTL. Indeed, when we calculated the average bias of the predicted genetic correlations, we observed a roughly 30% upward bias under loose linkage and an opposite 30% downward bias under pleiotropy (Figure S4). Additionally, though the bias in predicting genetic covariance was always negative, it was less so under loose linkage than under pleiotropy. This bias, particularly if uneven across predicted crosses, could lead to the observed

loss in accuracy. Practically, the impact of genetic architecture may be less important, since architecture is generally immutable and the effect on prediction accuracy is small (Figure 2).

Differences in the accuracy to predict the three parameters of a potential cross (i.e. mean, genetic variance, and genetic correlation) are attributable to the nature of each statistic and have practical implications. Greater accuracy when predicting the cross mean versus genetic variance was predicted by theory (Zhong and Jannink 2007) and has been observed empirically (Adeyemo and Bernardo 2019; Neyhart and Smith 2019); this trend is expected because the genetic variance, a second-order statistic, will be more adversely impacted by error in marker effect estimates. Similarly, the accuracy of the genetic correlation, a ratio of second-order statistics with large sampling variance (Robertson 1959), will be even more adversely affected. Even at large TP sizes, the predictions of the genetic correlation were only as accurate as those of the genetic variance at modest TP size and never as accurate as those of the cross mean (Figure 3). Practically, this suggests that very large TPs are needed for such predictions to be useful, a prospect that may be prohibitive for a plant breeder.

Informing cross selection by genetic correlations results in a greater multi-trait response

Under a simulated multi-trait recurrent selection scheme, we showed that the long-term genetic gain for two traits was greatest when crosses were selected on predicted correlated/superior progeny means (CPM). This was true under nearly all conditions of genetic architecture, trait heritability, and starting genetic correlation (Figure 4). Pointedly, we observed that a higher response was achieved even when the genetic correlation was negative (i.e. unfavorable), circumstances that might be common in a breeding program. Cross selection based on CPM was superior to selection on the predicted cross mean (FM) or random mating, standard choices in

programs using “best-by-best” breeding for cultivar development or in recurrent selection (Bernardo 2010).

The greater multi-trait selection response achieved under CPM cross selection can be attributed to many drivers, including genetic variance and correlation, haplotype and allele frequencies, and linkage disequilibrium (LD). We discuss their impacts below. Compared to FM, selection on CPM led to a higher maintenance of genetic variance for both traits (Figure 5A). When selecting on CPM, particularly at the relatively high selection intensity used in our simulation (i = 0.05; k_{sp} = 2.06), more weight is given to the predicted genetic variance versus the predicted mean (Equations 4 and 5). Segregation of QTL is explicitly driving the prediction of genetic variance in our approach, and an emphasis on variance may keep small or moderate-effect QTL at intermediate frequency, at which variance is maximized (Lynch and Walsh 1998). Therefore, when selecting on CPM, we might expect a short-term sacrifice of genetic gain for long-term benefit. Indeed, we note a small deficit in selection response in the first two breeding cycles relative to FM selection (Figure 4), the latter likely emphasizing the rapid increase in frequency of beneficial alleles at large and moderate-effect QTL, leading to fixation of unfavorable small-effect QTL due to drift or linkage (Figure 6B). Practically, the maintenance of genetic variance under CPM selection suggests that genetic gain may be sustained beyond 10 breeding cycles, as indicated by the implied trajectory of many of the observed response curves (Figure 4).

In addition to maintaining genetic variance, selection on CPM also sustained a more favorable genetic correlation in the breeding population (Figure 5B). In the first breeding cycle, under all selection methods, we observe a sharp trend towards more negative genetic correlations. This is attributable to a production of negative covariance due to LD (Felsenstein

1965; Bulmer 1971; Falconer and Mackay 1996) and the simultaneous fixation of favorable haplotypes or QTL and maintenance of antagonistic haplotypes or QTL at intermediate frequency (Bennett and Swiger 1980; Falconer and Mackay 1996). The long-term maintenance of more favorable genetic correlation may be due to similar forces influencing the genetic variance. Selection on CPM combined with stronger selection intensity weighs the predicted genetic correlation and genetic variance of each trait (Equations 4 and 5). As above, this would value the maintenance of segregating QTL in the population, in agreement with our observations (Figure 6B). Co-segregating QTL for both traits would impact the genetic covariance to a greater degree than the genetic variances (Bohren *et al.* 1966), leading to the observed differences in genetic correlation (Figure 5B). We would expect the linkage maintaining covariance in the short-term to be broken down by recombination, which may help explain why the higher correlation preserved by selection on CPM was marginally less under the loose linkage genetic architecture (Figure 5B).

The general trends in genetic correlation over cycles can be explained by the genetic architecture. With pleiotropy, the movement towards – or maintenance of – a negative correlation is due to the fixation of favorable QTL and presence of antagonistic QTL. Absent pleiotropy, the correlation is due entirely to LD (Lande 1984; Lynch and Walsh 1998), which is degraded by recombination, eventually moving the genetic correlation towards zero (Villanueva and Kennedy 1990). Though our results confirm this under the loose linkage and tight linkage architecture (Figure 5B), the final genetic correlation is slightly negative, and more so with tight linkage. This is likely due to fixation of antagonistic QTL haplotypes, which, particularly when tightly linked, can effectively act as pleiotropic loci (Lande 1984) and are subject to the same competing forces mentioned earlier.

Implementation in a breeding program

To demonstrate its feasibility under more realistic conditions, we generated predictions of genetic correlations among populations in a barley breeding program. For two pairs of traits with moderately or strongly unfavorable correlations, we identified many crosses with favorable predicted correlations (Figure 7, Table 2), suggesting that specific crosses could be targeted to improve multiple traits simultaneously. This would rely on accurately discriminating among crosses, and we attempted to validate predictions of genetic correlations using empirical data of breeding populations.

Though we were only able to validate predictions for one pair of traits (Table 3), we observed that predictive ability seemed to be associated with the heritability of both traits, in agreement with the results from our first simulation. Of course, trait heritability may influence accuracy beyond unreliable marker effect estimates. With less heritable traits, the correlation among environmental effects is expected to have a greater influence on the phenotypic correlation (Lynch and Walsh 1998). It is not difficult to imagine how shared environment could influence the observed correlations. For instance, environmental stresses might stunt the growth of plants and promote earlier flowering, creating a positive correlation between these traits. Additionally, plants that flower later or are taller may avoid the soil-borne *Fusarium graminearum* inoculum, potentially leading to artificial negative correlations between the traits. The results of our simulations and empirical experiment confirm that, as in any other implementation of genomewide selection, reliable phenotypic data is paramount.

The modest size of our TP (n = 175) likely constrained prediction accuracy, as suggested in our first simulation (Figure 2). Previous genomewide selection research, including those focused on barley, suggest a pattern of diminishing returns when predicting line means with

ever-larger TPs (Lorenz *et al.* 2012; Sallam *et al.* 2015). A breeding program using a smaller TP, perhaps as a resource-saving measure, may be ill-equipped to utilize predictions of genetic correlations. The size of our TP was a function of the early stage of implementing genomewide selection in the breeding program, and we might expect that as more individuals are phenotyped and genotyped, the size of the training dataset will become more satisfactory.

Fortunately, the barrier for a breeder to incorporate predictions of genetic correlations is low. First, the data required for predictions (phenotypes, marker genotypes, and a genetic map) are commonly available in many breeding programs. Second, it is relatively inexpensive, in both time and computing power, to generate such predictions. Thus, it is possible that this procedure can be an additional tool for breeders to make decisions. We note, however, that validating predictions of genetic correlations requires phenotypic data on many large families, leading to population sizes that are generally unrealistic for a breeding program (Bernardo 2010). It is likely that these predictions, if implemented, will not be routinely validated, unlike genomewide predictions of genotypic means, and this lack of feedback may prove discouraging for breeders. Nevertheless, further work is necessary to demonstrate empirically the utility of selecting crosses informed by predictions of genetic correlations, with emphasis on the response to selection for two potentially unfavorably correlated traits.

ACKNOWLEDGEMENTS

We thank Ed Schiefelbein, Guillermo Velasquez, and Karen Beaubien for technical support during population development, phenotypic data collection, and genotyping. Thanks go to Ruth Dill-Macky for suppling *Fusarium graminearum* inoculum for St. Paul and to Madeline Smith and Joseph Wodarek for managing the FHB trial in Crookston, MN. We are grateful to Austin Case, Jo Heuschele, John Hill Price, Ian McNish, Becky Zhong, and Alexander Susko for assistance and encouragement. Resources from the Minnesota Supercomputing Institute were used to complete this project. This research was supported by the U.S. Wheat and Barley Scab Initiative, the Minnesota Department of Agriculture, Rahr Malting Company, the Brewers Association, the American Malting Barley Association, and USDA-NIFA Grant #2018-67011-28075.

REFERENCES

Adeyemo E., and R. Bernardo, 2019 Predicting Genetic Variance from Genomewide Marker Effects Estimated from a Diverse Panel of Maize Inbreds. Crop Sci. 59: 1–8. https://doi.org/10.2135/cropsci2018.08.0525

Allier A., L. Moreau, A. Charcosset, S. Teyssèdre, and C. Lehermeier, 2019 Usefulness Criterion and post-selection Parental Contributions in Multi-parental Crosses: Application to Polygenic Trait Introgression. G3 Genes|Genomes|Genetics. https://doi.org/https://doi.org/10.1534/g3.119.400129

Bandillo N., D. Jarquin, Q. Song, R. Nelson, P. Cregan, *et al.*, 2015 A Population Structure and Genome-Wide Association Analysis on the USDA Soybean Germplasm Collection. Plant Genome 8. https://doi.org/10.3835/plantgenome2015.04.0024

Bennett G. L., and L. A. Swiger, 1980 Genetic variance and correlation after selection for two traits by index, independent culling levels, and extreme selection. Genetics 763–775.

Bernardo R., 2010 *Breeding for Quantitative Traits in Plants*. Stemma Press, Woodbury, Minnesota.

Bernardo R., 2014 Genomewide Selection of Parental Inbreds: Classes of Loci and Virtual Biparental Populations. Crop Sci. 54: 2586. https://doi.org/10.2135/cropsci2014.01.0088

Beyene Y., K. Semagn, S. Mugo, A. Tarekegne, R. Babu, *et al.*, 2015 Genetic Gains in Grain Yield Through Genomic Selection in Eight Bi-parental Maize Populations under Drought Stress. Crop Sci. 55: 154–163. https://doi.org/10.2135/cropsci2014.07.0460

Blake V. C., C. Birkett, D. E. Matthews, D. L. Hane, P. Bradbury, *et al.*, 2016 The Triticeae Toolbox: Combining Phenotype and Genotype Data to Advance Small-Grains Breeding. Plant Genome 9: 1–10. https://doi.org/10.3835/plantgenome2014.12.0099

Bohn M., H. F. Utz, and A. E. Melchinger, 1999 Genetic Similarities among Winter Wheat Cultivars Determined on the Basis of RFLPs, AFLPs, and SSRs and Their Use for Predicting Progeny Variance. Crop Sci. 39: 228. https://doi.org/10.2135/cropsci1999.0011183X003900010035x

Bohren B. B., W. G. Hill, and A. Robertson, 1966 Some observations on asymmetrical correlated responses to selection. Genet. Res. (Camb). 7: 44–57.

Boyle E. A., Y. I. Li, and J. K. Pritchard, 2017 An Expanded View of Complex Traits : From Polygenic to Omnigenic. Cell 169: 1177–1186. https://doi.org/10.1016/j.cell.2017.05.038

Broman K. W., H. Wu, S. Sen, and G. A. Churchill, 2003 R/qtl: QTL mapping in experimental crosses. Bioinformatics 19: 889–890. https://doi.org/10.1093/bioinformatics/btg112

Bulik-Sullivan B., H. K. Finucane, V. Anttila, A. Gusev, F. R. Day, *et al.*, 2015 An atlas of genetic correlations across human diseases and traits. Nat. Genet. 47: 1236–1241. https://doi.org/10.1038/ng.3406

Bulmer M. G., 1971 The Effect of Selection on Genetic Variability. Am. Nat. 105: 201–211. https://doi.org/10.1086/282718

Calus M. P. L., and R. F. Veerkamp, 2011 Accuracy of multi-trait genomic selection using different methods. Genet. Sel. Evol. 43: 1–14.

Chi R. K., S. A. Eberhart, and L. H. Penny, 1969 Covariances Among Relatives in a Maize Variety (Zea Mays L.). Genetics 63: 511–520.

Close T. J., P. R. Bhat, S. Lonardi, Y. Wu, N. Rostoks, *et al.*, 2009 Development and implementation of high-throughput SNP genotyping in barley. BMC Genomics 10. https://doi.org/10.1186/1471-2164-10-582

Combs E., and R. Bernardo, 2013 Genomewide selection to introgress semidwarf maize

germplasm into US Corn Belt inbreds. Crop Sci. 53: 1427–1436. https://doi.org/10.2135/cropsci2012.11.0666

Daetwyler H. D., B. Villanueva, and J. A. Woolliams, 2008 Accuracy of predicting the genetic risk of disease using a genome-wide approach. PLoS One 3. https://doi.org/10.1371/journal.pone.0003395

Deng Y., and W. Pan, 2017 Testing Genetic Pleiotropy with GWAS Summary Statistics for Marginal and Conditional Analyses. Genetics 207: 1285–1299.

Falconer D. S., and T. F. C. Mackay, 1996 *Introduction to Quantitative Genetics*. Pearson Prentice Hall, Harlow, Essex, UK.

Felsenstein J., 1965 The Effect of Linkage on Directional Selection. Genetics 52: 349–363.

Fisher R. A., 1919 The Correlation between Relatives on the Supposition of Mendelian Inheritance. Trans. R. Soc. Edinburgh 52: 399–433. https://doi.org/doi:10.1017/S0080456800012163

Habier D., R. L. Fernando, K. Kizilkaya, and D. J. Garrick, 2011 Extension of the bayesian alphabet for genomic selection. BMC Bioinformatics 12: 186. https://doi.org/10.1186/1471-2105-12-186

Hazel L. N., 1943 The Genetic Basis for Constructing Selection Indexes. Genetics 28: 476–490.

Jia Y., and J.-L. Jannink, 2012 Multiple-Trait Genomic Selection Methods Increase Genetic Value Prediction Accuracy. Genetics 192: 1513–1522. https://doi.org/10.1534/genetics.112.144246

Korte A., B. J. Vilhjálmsson, V. Segura, A. Platt, Q. Long, *et al.*, 2012 A mixed-model approach for genome-wide association studies of correlated traits in structured populations. Nat. Genet. 44: 1066–71. https://doi.org/10.1038/ng.2376

Lande R., 1984 The genetic correlation between characters maintained by selection, linkage and inbreeding. Genet. Res. (Camb). 44: 309. https://doi.org/10.1017/S0016672300026549

Lee S. H., J. Yang, M. E. Goddard, P. M. Visscher, and N. R. Wray, 2012 Estimation of pleiotropy between complex diseases using single-nucleotide polymorphism-derived genomic relationships and restricted maximum likelihood. Bioinformatics 28: 2540–2542. https://doi.org/10.1093/bioinformatics/bts474

Lehermeier C., S. Teyssèdre, and C.-C. Schön, 2017 Genetic Gain Increases by Applying the Usefulness Criterion with Improved Variance Prediction in Selection of Crosses. Genetics 207: genetics.300403.2017. https://doi.org/10.1534/genetics.117.300403

Lian L., A. Jacobson, S. Zhong, and R. Bernardo, 2015 Prediction of genetic variance in biparental maize populations: Genomewide marker effects versus mean genetic variance in prior populations. Crop Sci. 55: 1181–1188. https://doi.org/10.2135/cropsci2014.10.0729

Lorenz A. J., K. P. Smith, and J.-L. Jannink, 2012 Potential and Optimization of Genomic Selection for Fusarium Head Blight Resistance in Six-Row Barley. Crop Sci. 52: 1609–1621. https://doi.org/10.2135/cropsci2011.09.0503

Lynch M., and B. Walsh, 1998 *Genetics and Analysis of Quantitative Traits*. Sinauer Associates, Inc., Sunderland, MA, USA.

Mackay T. F. C., 2010 Mutations and quantitative genetic variation: Lessons from Drosophila. Philos. Trans. R. Soc. B 365: 1229–1239. https://doi.org/10.1098/rstb.2009.0315

Meuwissen T. H. E., B. J. Hayes, and M. E. Goddard, 2001 Prediction of total genetic value using genome-wide dense marker maps. Genetics 157: 1819–1829. https://doi.org/11290733

Mohammadi M., T. Tiede, and K. P. Smith, 2015 PopVar: A Genome-Wide Procedure for

Predicting Genetic Variance and Correlated Response in Biparental Breeding Populations. Crop Sci. 55: 2068–2077. https://doi.org/10.2135/cropsci2015.01.0030

Muñoz-Amatriaín M., M. J. Moscou, P. R. Bhat, J. T. Svensson, J. Bartoš, *et al.*, 2011 An Improved Consensus Linkage Map of Barley Based on Flow-Sorted Chromosomes and Single Nucleotide Polymorphism Markers. Plant Genome J. 4: 238–249. https://doi.org/10.3835/plantgenome2011.08.0023

Neyhart J. L., and K. P. Smith, 2019 Validating Genomewide Predictions of Genetic Variance in a Contemporary Breeding Program. Crop Sci. in press.

Osthushenrich T., M. Frisch, and E. Herzog, 2017 Genomic selection of crossing partners on basis of the expected mean and variance of their derived lines, (A. Zhang, Ed.). PLoS One 12. https://doi.org/10.1371/journal.pone.0188839

R Core Team, 2018 R: A language and environment for statistical computing

Robertson A., 1959 The Sampling Variance of the Genetic Correlation Coefficient. Biometrics 15: 469–485.

Sallam A. H., J. B. Endelman, J.-L. Jannink, and K. P. Smith, 2015 Assessing Genomic Selection Prediction Accuracy in a Dynamic Barley Breeding Population. Plant Genome 8. https://doi.org/10.3835/plantgenome2014.05.0020

Schaid D. J., X. Tong, B. Larrabee, R. B. Kennedy, G. A. Poland, *et al.*, 2016 Statistical methods for testing genetic pleiotropy. Genetics 204: 483–497. https://doi.org/10.1534/genetics.116.189308

Schnell F. W., and H. F. Utz, 1975 F1-leistung und elternwahl euphyder züchtung von selbstbefruchtern, pp. 243–248 in *Bericht über die Arbeitstagung der Vereinigung Österreichischer Pflanzenzüchter*, BAL Gumpenstein, Gumpenstein, Austria.

Simmonds N. W., 1995 The relation between yield and protein in cereal grain. J. Sci. Food Agric. 67: 309–315. https://doi.org/10.1002/jsfa.2740670306

Sleper J. A., and R. Bernardo, 2018 Genomewide selection for unfavorably correlated traits in maize. Crop Sci. 58: 1587–1593. https://doi.org/10.2135/cropsci2017.12.0719

Souza E., and M. E. Sorrells, 1991 Prediction of progeny variation in oat from parental genetic relationships. Theor. Appl. Genet. 82: 233–241. https://doi.org/10.1007/BF00226219

Tiede T., L. Kumar, M. Mohammadi, and K. P. Smith, 2015 Predicting genetic variance in bi-parental breeding populations is more accurate when explicitly modeling the segregation of informative genomewide markers. Mol. Breed. 35: 199. https://doi.org/10.1007/s11032-015-0390-6

Tiede T., and K. P. Smith, 2018 Evaluation and retrospective optimization of genomic selection for yield and disease resistance in spring barley. Mol. Breed. 38. https://doi.org/10.1007/s11032-018-0820-3

Utz H. F., M. Bohn, and A. E. Melchinger, 2001 Predicting progeny means and variances of winter wheat crosses from phenotypic values of their parents. Crop Sci. 41: 1470–1478. https://doi.org/10.2135/cropsci2001.4151470x

Villanueva B., and B. W. Kennedy, 1990 Effect of selection on genetic parameters of correlated traits. Theor Appl Genet 80: 746–752. https://doi.org/10.1007/BF00224187

Wimmer V., C. Lehermeier, T. Albrecht, H. J. Auinger, Y. Wang, *et al.*, 2013 Genome-wide prediction of traits with different genetic architecture through efficient variable selection. Genetics 195: 573–587. https://doi.org/10.1534/genetics.113.150078

Zhong S., and J. L. Jannink, 2007 Using quantitative trait loci results to discriminate among crosses on the basis of their progeny mean and variance. Genetics 177: 567–576.

https://doi.org/10.1534/genetics.107.075358

FIGURE CAPTIONS

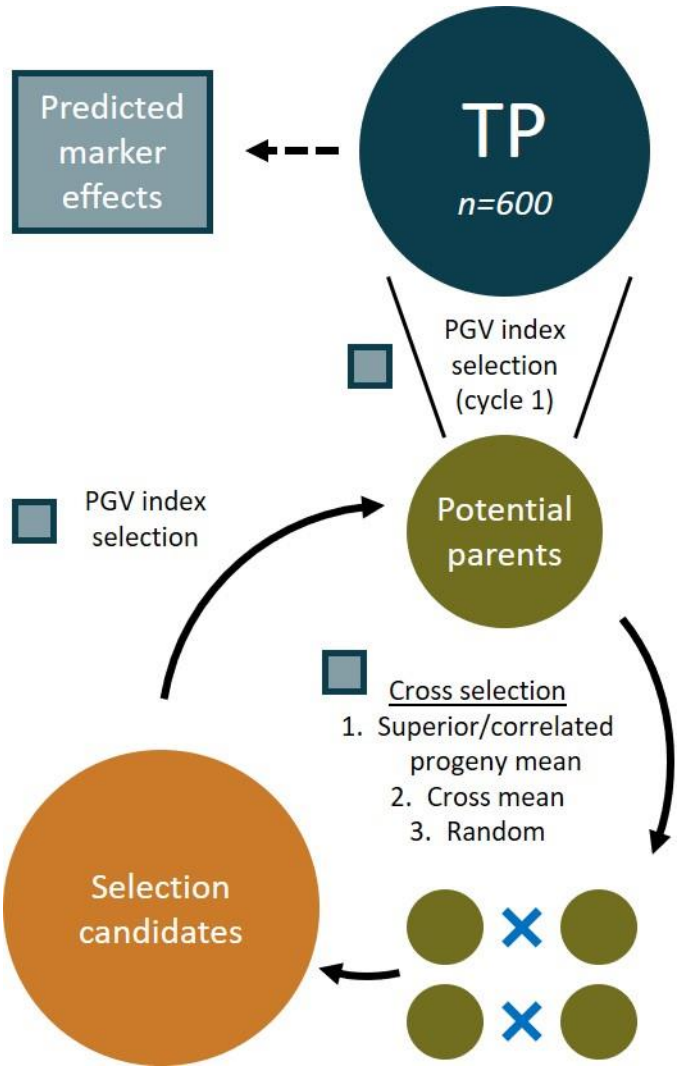

Figure 1. Scheme outlining the recurrent selection simulation (Simulation 2). A training population (TP) was first sampled and used to predict genomewide marker effects. In the first cycle, potential parents were selected from the TP using a multi-trait index of predicted genotypic values (PGVs). Crosses between potential parents were selected by one of three methods. Selected crosses were used to simulate selection candidates, which underwent PGV index selection, leading to potential parents of the next cycle. Ten breeding cycles were simulated. Any processes that relied on the predicted marker effects are noted with a blue/grey box.

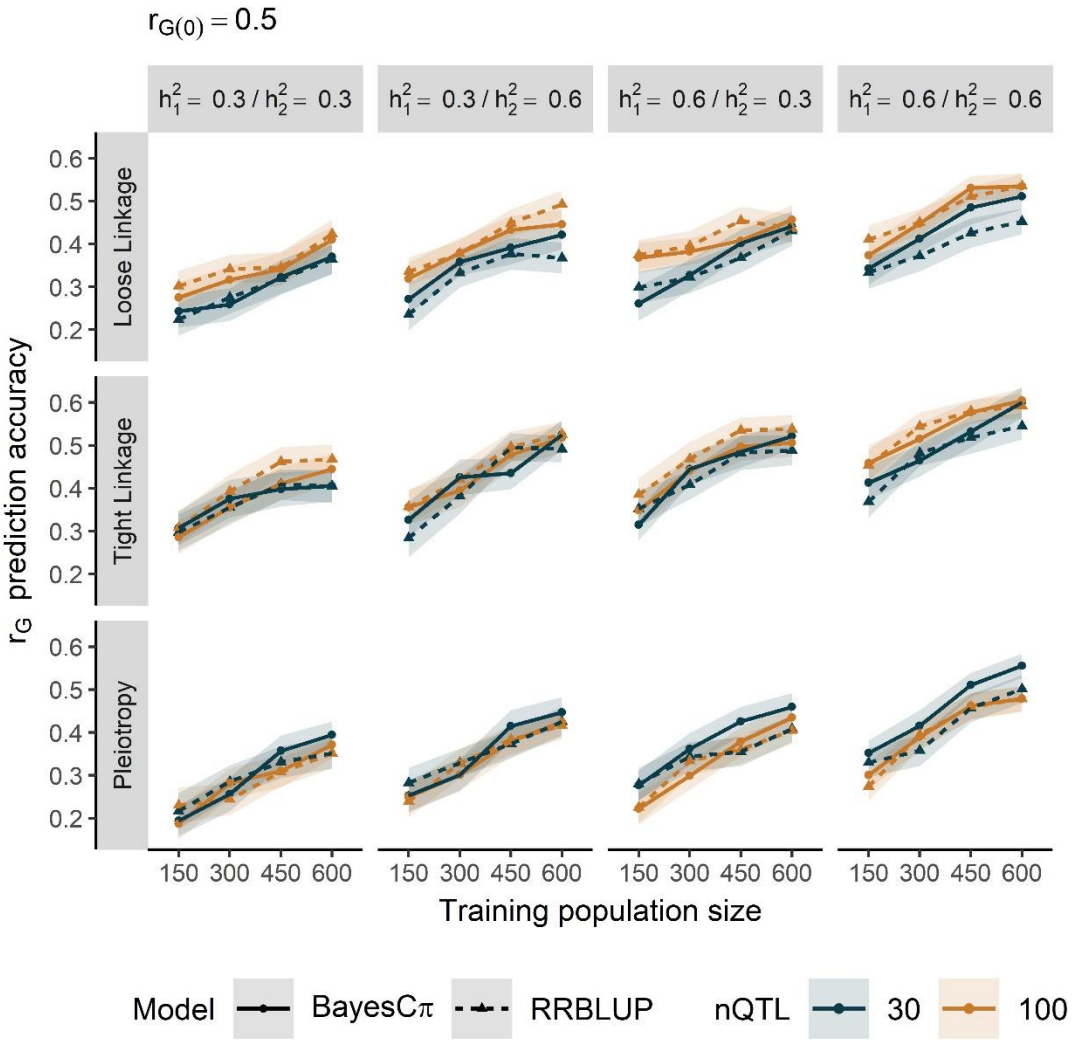

Figure 2. The prediction accuracy of the genetic correlation in a cross increased with larger training populations and greater trait heritability. Accuracy was also influenced by genetic correlation architecture (loose linkage, tight linkage, or pleiotropy), prediction model [BayesCπ (solid) or RRBLUP (dashed)], and number of QTL [30 (navy) or 100 (orange)]. Lines denote the mean of 100 simulation replicates, and ribbons denote a 95% confidence interval. Results are restricted to a base genetic correlation of 0.5. (See Figure S3 and Table S1 for complete results.)

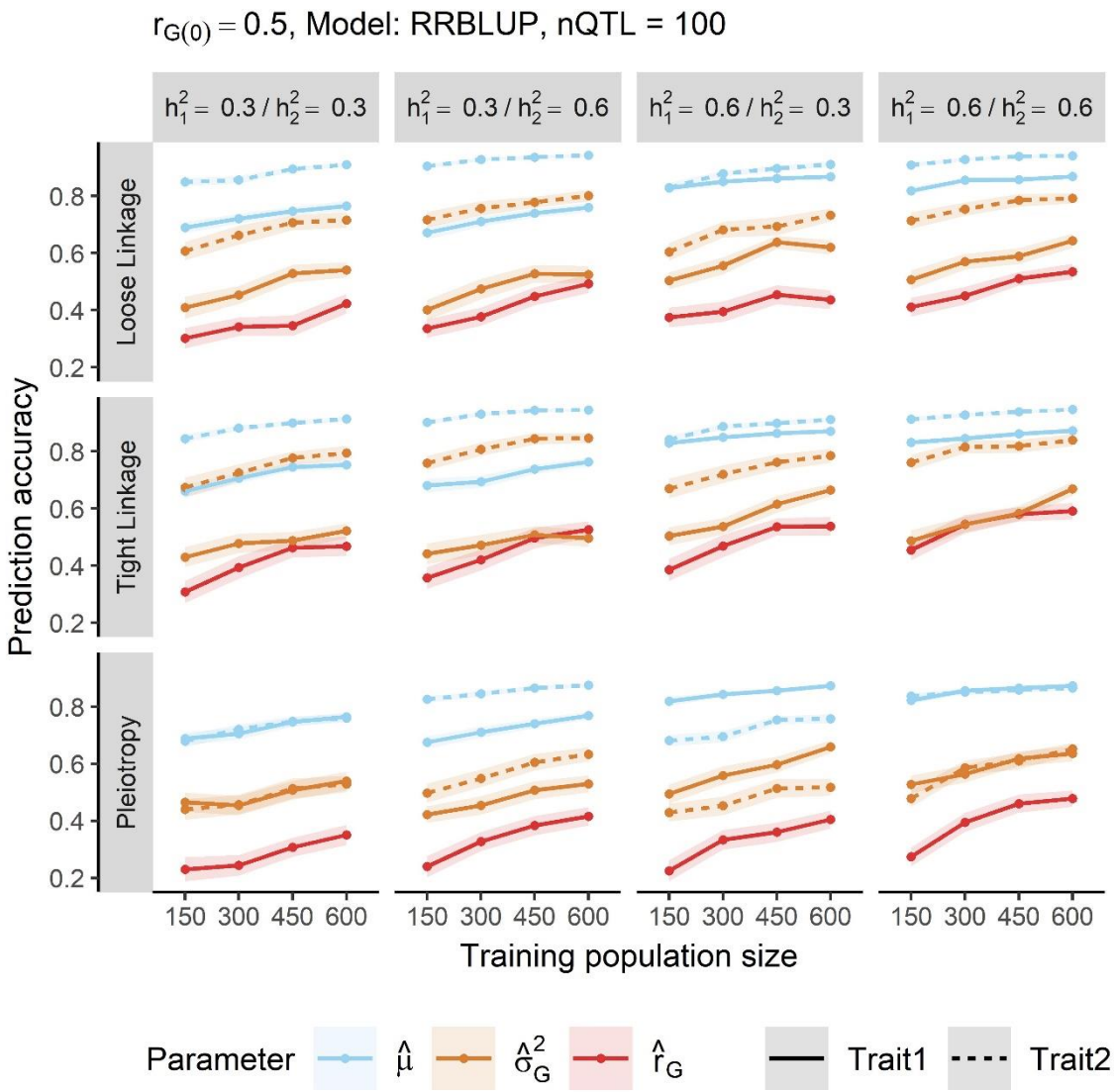

Figure 3. Parameters of a cross were predicted with varying degrees of accuracy in our simulation. Predictions of the cross mean ($\hat{\mu}$, blue) were most accurate, followed by genetic variance ($\hat{\sigma}_G^2$, orange) and genetic correlation ($\hat{r}_G$, red); this ranking was consistent across trait heritabilities, training population size, and genetic correlation architecture (loose linkage, tight linkage, or pleiotropy). Lines denote the mean of 100 simulation replicates, and ribbons denote a 95% confidence interval. Results are restricted to a base genetic correlation of 0.5, RRBLUP prediction model, and 100 QTL. (See Table S1 for complete results.)

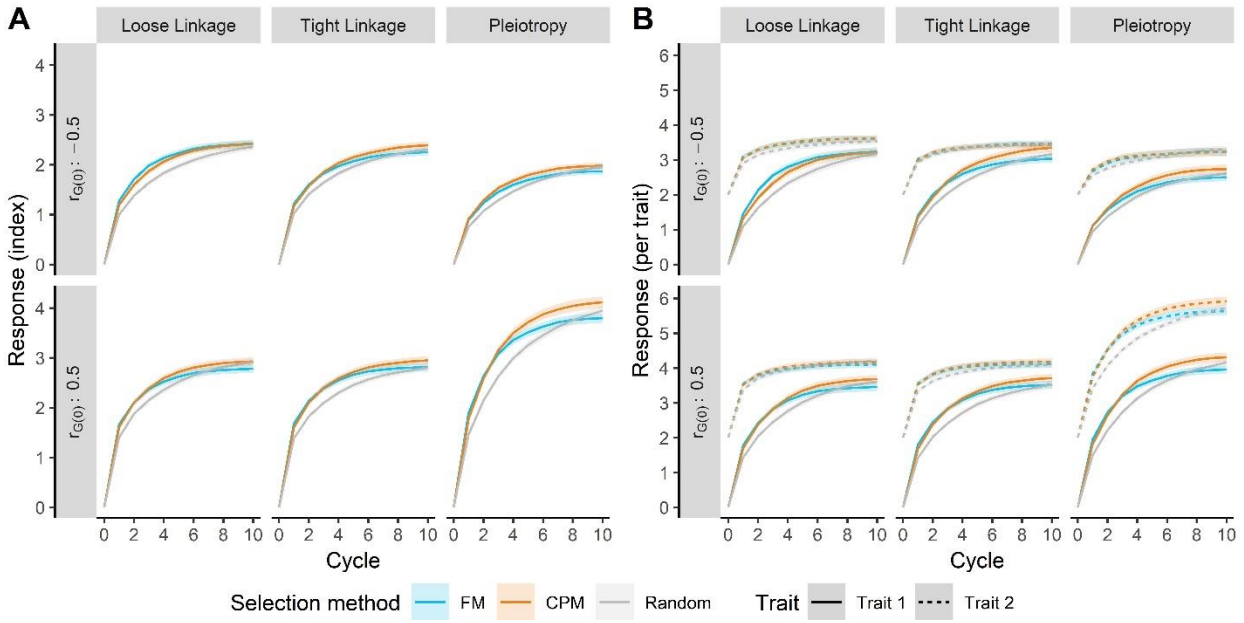

Figure 4. Selecting crosses on the predicted correlated/superior progeny mean (CPM, orange) led to a greater long-term response (in units of genetic standard deviations) compared to selection on the predicted family mean (FM), blue) or by random selection (grey). This was true for a two-trait index (**A**) and, generally, both traits individually (**B**) across three correlation architectures and two base genetic correlations ($r_{G(0)}$). Lines denote the mean of 250 simulation replicates, and the ribbon denotes a 95% confidence interval. To improve readability, the response values for Trait 2 in (**B**) were nudged upwards by 2 units.

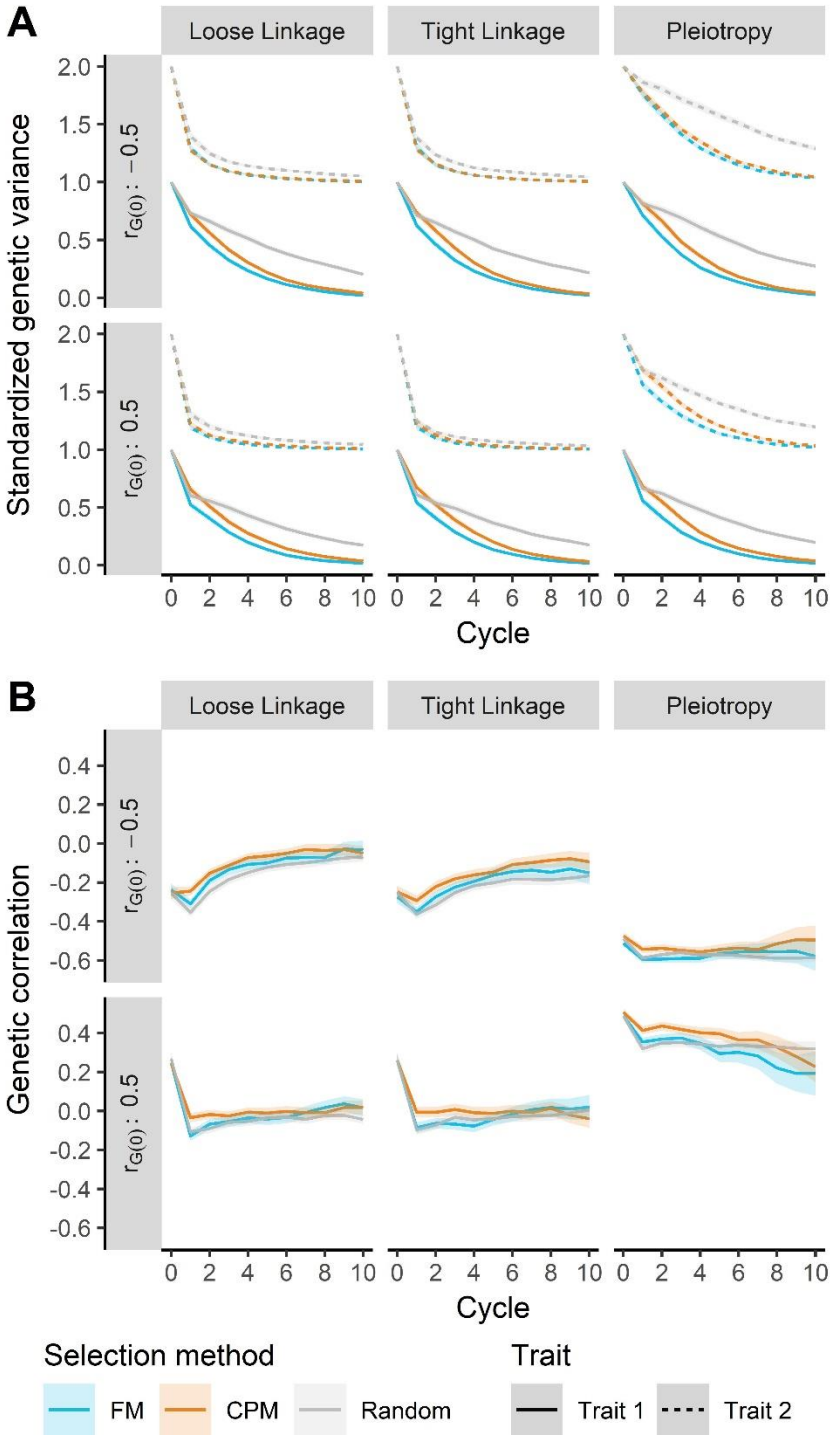

Figure 5. Variance components in the simulated breeding population were influenced by the cross selection method (family mean, FM, blue; correlated/superior progeny mean, CPM, orange; random, grey), genetic architecture, and base genetic correlation ($r_{G(0)}$). (**A**) The genetic variances (measured as the proportion of base genetic variance) of trait 1 (solid) and trait 2 (dashed) declined over breeding cycles, but the rate depended on the cross selection method. (**B**) The genetic correlation was typically more positive (i.e. favorable) when selecting crosses on CPM. Lines denote the mean of 250 simulation replicates, and the ribbon denotes a 95% confidence interval. To improve readability, the genetic variance values for trait 2 in (**A**) were nudged upwards by 1 unit.

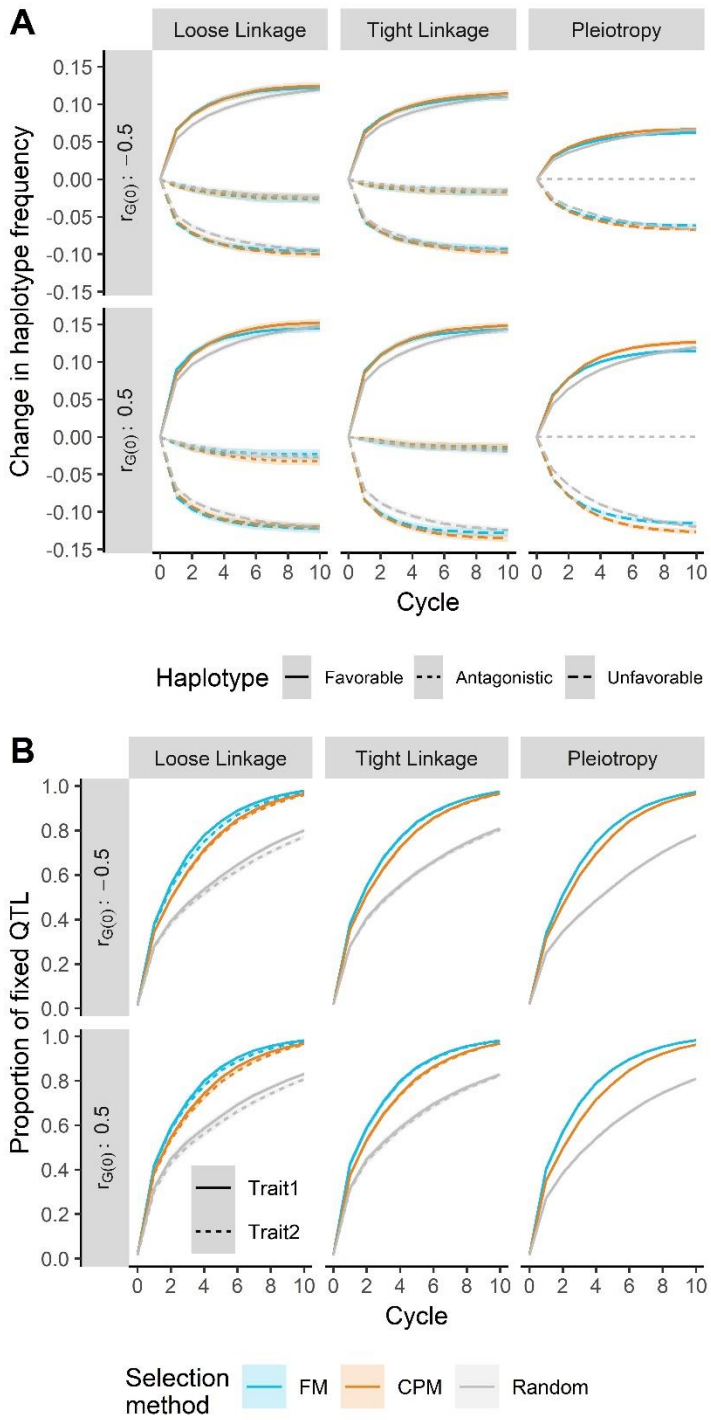

Figure 6. The change in frequency of two-trait quantitative trait locus (QTL) haplotypes and proportion of fixed QTL depended on the cross selection method genetic architecture, and base genetic correlation ($r_{G(0)}$). (**A**) The increase in frequency of favorable (solid) haplotypes and decrease in frequency of unfavorable (dashed) and antagonistic (dotted) haplotypes was often greater when selecting crosses on the correlated/superior progeny mean (CPM, orange). (**B**) The rate of QTL fixation for both trait 1 (solid) and trait 2 (dotted) was always greatest with cross selection on the family mean (FM, blue), followed by CPM and random mating (grey). Lines denote the mean of 250 simulation replicates, and the ribbon denotes a 95% confidence interval.

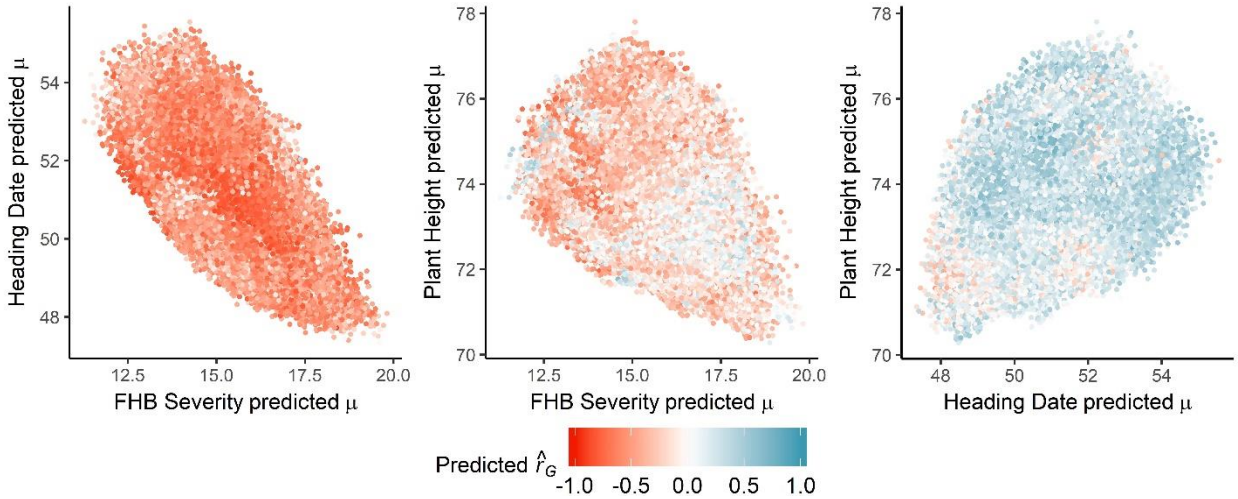

Figure 7. In the barley breeding population used to empirically validate predictions, the relationship between the predicted cross means ($\hat{\mu}$) of three pairs of traits for *n* = 330,078 potential crosses mirrored the overall distribution of predicted genetic correlations ($\hat{r}_G$), shaded from red (negative) to blue (positive). FHB, *Fusarium* head blight.

TABLE CAPTIONS

Table 1. In our two simulation experiments, we modified the heritability (h^2) and number of quantitative trait loci (N_{QTL}) of two traits, the starting genetic correlation ($r_{G(0)}$), correlation architecture, size of a training population (N_{TP}), and model used to predicted genomewide marker effects.

Simulation experiment	h^2	N_{QTL}	$r_{G(0)}$	Correlation architecture	N_{TP}	Model
Experiment 1 (prediction accuracy)	Trait 1: 0.3, 0.6, 1 Trait 2: 0.3, 0.6, 1	30, 100	-0.5, 0, 0.5	Pleiotropy Tight linkage Loose linkage	150, 300, 450, 600	RR-BLUP BayesCπ
Experiment 2 (long-term response)	Trait 1: 0.6 Trait 2: 0.3, 0.6	100	-0.5, 0.5	Pleiotropy Tight linkage Loose linkage	600	RR-BLUP

Table 2. Estimated genetic correlation in the empirical barley training population ($\hat{r}_{G(TP)}$) and the mean and range of the predicted genetic correlations among 330,078 potential crosses ($\hat{r}_{g(PC)}$) for three pairs of quantitative traits

Trait 1	Trait 2	$\hat{r}_{G(TP)}$	Mean (range) of $\hat{r}_{g(PC)}$
FHB[a] Severity	Heading Date	-0.99	-0.54 (-0.94, 0.52)
FHB Severity	Plant Height	-0.61	-0.26 (-0.86, 0.63)
Heading Date	Plant Height	0.38	0.24 (-0.73, 0.87)

[a]*Fusarium* head blight

Table 3. Number of phenotyped validation families, mean (and range) of observed genetic correlations, and the predictive ability, measured as the correlation between the predicted ($\hat{r}_g$) and observed (r_G) genetic correlation, for each of three pairs of traits. A 95% confidence interval for the predictive ability was estimated from 1,000 bootstrapping replicates.

Trait 1	Trait 2	N_f[b]	Mean (range) of r_G	$cor(\hat{r}_g, r_G)$
FHB[a] Severity	Heading Date	14	-0.18 (-0.72, 0.58)	0.24 (-0.30, 0.70)
FHB Severity	Plant Height	14	-0.038 (-0.67, 0.64)	-0.012 (-0.53, 0.59)
Heading Date	Plant Height	26	-0.13 (-0.64, 0.69)	0.41* (0.024, 0.71)

[a]*Fusarium* head blight
[b]Number of families used to compute predictive ability
*Significant at $P < 0.05$